Supplementary Materials

Piezoelectric-Driven Fenton System Based on Bismuth Ferrite Nanosheets for Removal of *N*-acetyl-para-aminophenol in Aqueous Environments

Chi Zhou [1,†], Shenglong Jing [2,†], Teng Miao [1], Nianlai Zhou [1], Hang Zhang [1], Yi Zhang [1], Lin Ge [2], Wencheng Liu [2] and Zixin Yang [2,*]

[1] Hubei Water Resources and Hydropower Science and Technology Promotion Center, Hubei Water Resources Research Institute, Wuhan 430070, China

[2] Department of chemistry, College of Chemistry, Huazhong Agricultural University, Wuhan 430070, China

* Correspondence: zixinyang@mail.hzau.edu.cn

[†] These authors contributed equally to this work.

Ultrasonic-conductivity response curve

To explore the ability of BFO to produce piezoelectric electrons under ultrasound, Cr (VI) was selected as the target substrate for piezo-reduction. Experimental device was shown as Figure S5a, the conductivity of Cr (VI) solution was measured by the DDS-11A electrical conductivity meter. Adding 50 mg of piezo-catalyst to 50 mL of 10 mg/L Cr (VI) solution (pH=2.0 potassium dichromate solution), stirring 30 min to complete the adsorption-desorption equilibrium between substrate and catalyst. Then, applying ultrasonic irradiation intermittent on the suspension with the power of 100% (300 W) or 50% (150 W). The change of conductivity over time was recorded as ultrasonic-conductivity response curve.

Cr (VI) reduction experiment

The diphenylcarbazide color method [1] was used to determine the exact concentration of Cr (VI) and calculate the degradation rate. Adding 50 mg of piezo-catalyst to 50 mL of 10 mg/L Cr (VI) solution (pH=2.0 potassium dichromate solution), stirring 30 min to complete the adsorption-desorption equilibrium between substrate and catalyst (Take 2 mL of sample every 10 min, Figure S6). Then, ultrasound was performed for 60 min (2 mL samples were taken every 15 min). Acquired samples were centrifuged, the content of Cr (VI)was determined by the diphenylcarbazide colorimetry method at 550 nm using a visible–ultraviolet spectrophotometer (Shimadzu UV-1800). Formula S1 was used for calculating Cr (VI) reduction rate:

$$Cr\ (VI)\ reduction\ rate = \frac{C_0 - C_t}{C_0} \times 100\% = \frac{A_0 - A_t}{A_0} \times 100\% \quad (S1)$$

where c_0 and c_t are the concentration of Cr (VI) at beginning of reaction and a given reaction time, respectively, A_0 and A_t are the absorbance of samples at 550 nm in the initial and a given reaction time respectively. In order to prove the cyclic stability of the catalyst, the piezoelectric materials were refreshed and repeated the same Cr (VI) reduction process three times. Further analysis revealed the reactions followed the first-order kinetic model:

$$ln\frac{c_t}{c_0} = -k_{obs} \times t \quad (S2)$$

where c_0 and c_t (mg·L^{-1}) are the concentration of Cr (VI) at beginning of reaction and a given reaction time, respectively, k_{obs} is the reaction rate constant and t is the reaction time, i.e., holding time of ultrasonic irradiation.

***N*-Acetyl-p-aminophenol (APAP) degradation experiment**

In order to investigate the oxidation ability of the catalyst under ultrasonic irradiation, APAP was used as the model substrate to evaluate the oxidation activity. The 50 mg catalyst was dispersed in 50 mL of 50 μmol/L APAP solution and stirred in the dark for 30 min (3 mL samples were taken every 10 min). Then, ultrasonic irradiating in dark for 60 min (3 mL of samples taken every 15 min), samples were centrifuged and filtered (PVDF, 0.22 μm) to take supernatant, and

the concentration of APAP in the supernatant was detected by HPLC (Agilent 1200, UV detector) and Calculated by Formula S3:

$$APAP\ reduction\ rate = \frac{C_0' - C_t'}{C_0'} \times 100\% = \frac{S_0 - S_t}{S_0} \times 100\% \quad (S3)$$

where C_0' and C_t' are the concentration of APAP at beginning of reaction and a given reaction time, respectively, S_0 and S_t are the absorption peak area of samples at 250 nm in the initial and a given reaction time respectively.
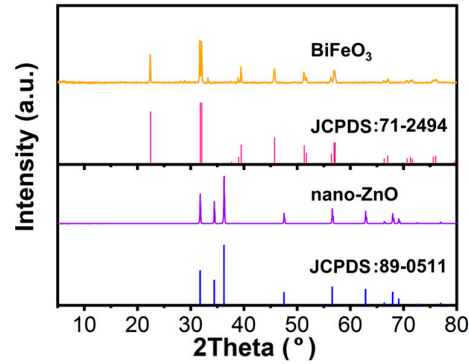
Figure S1. XRD patterns of the BiFeO₃ and nano-ZnO.
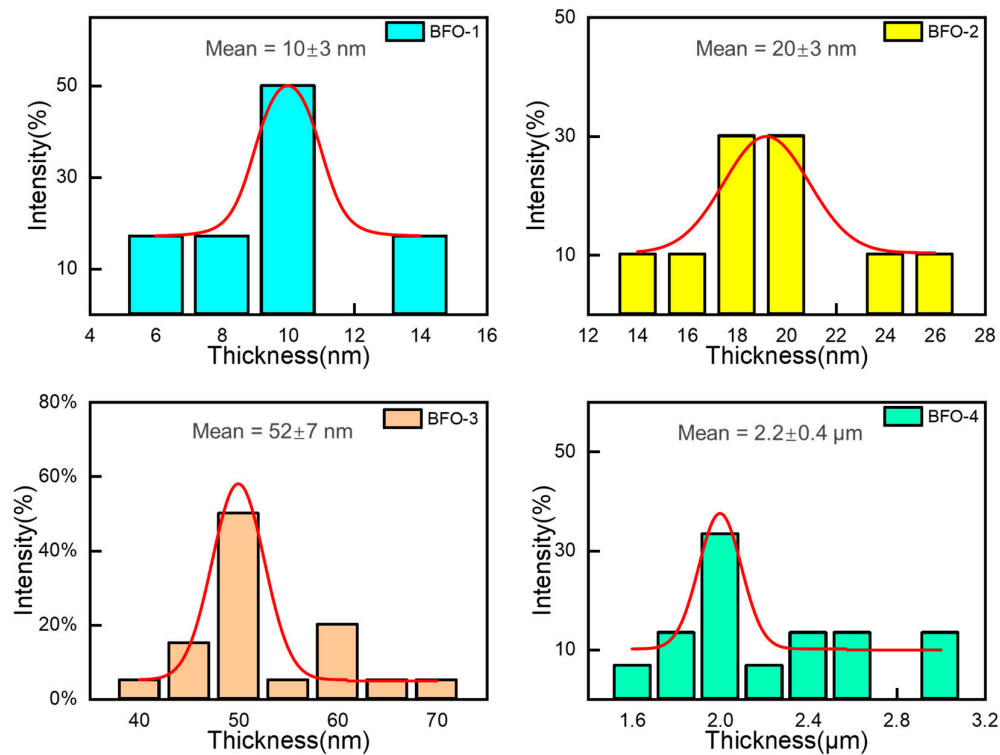
Figure S2. The thickness distribution and average value of BFO nanosheets. thickness mean values of BFO samples statistically obtained from their AFM results (BFO-1, BFO-2) or SEM results (BFO-3, BFO-4).
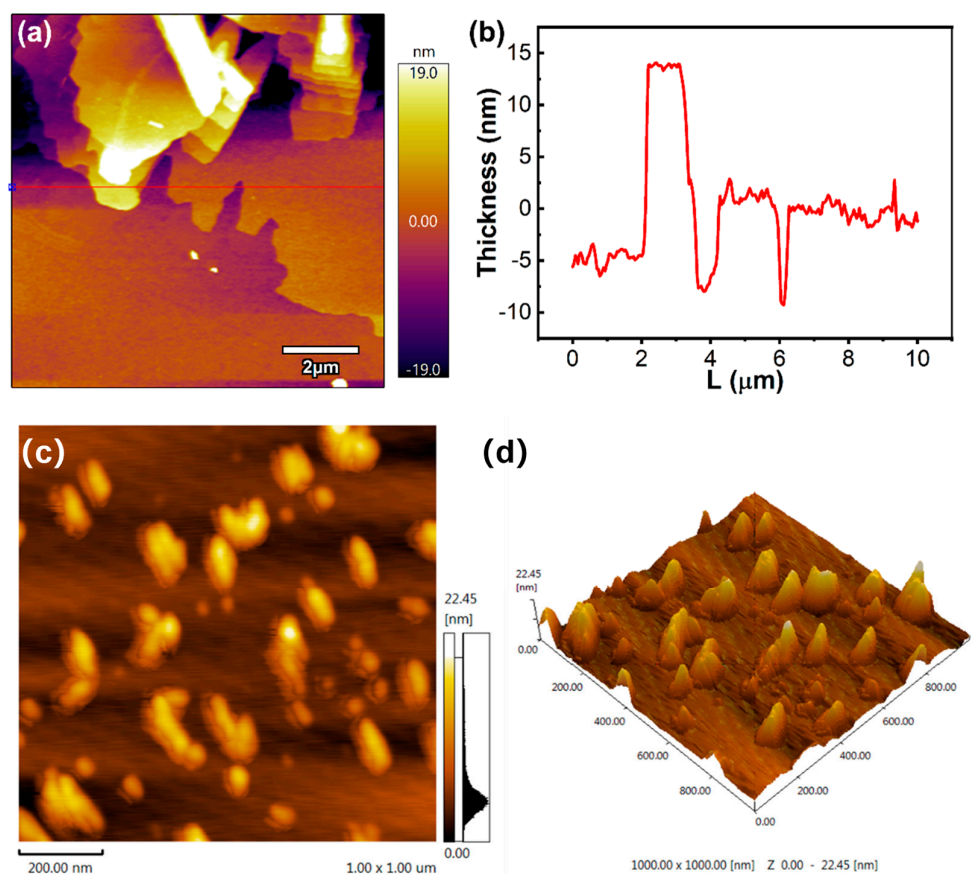
Figure S3. AFM image of BFO-1(a) and the corresponding thickness at the red line (b); 2D (c) and 3D (d) AFM images of BFO-2.
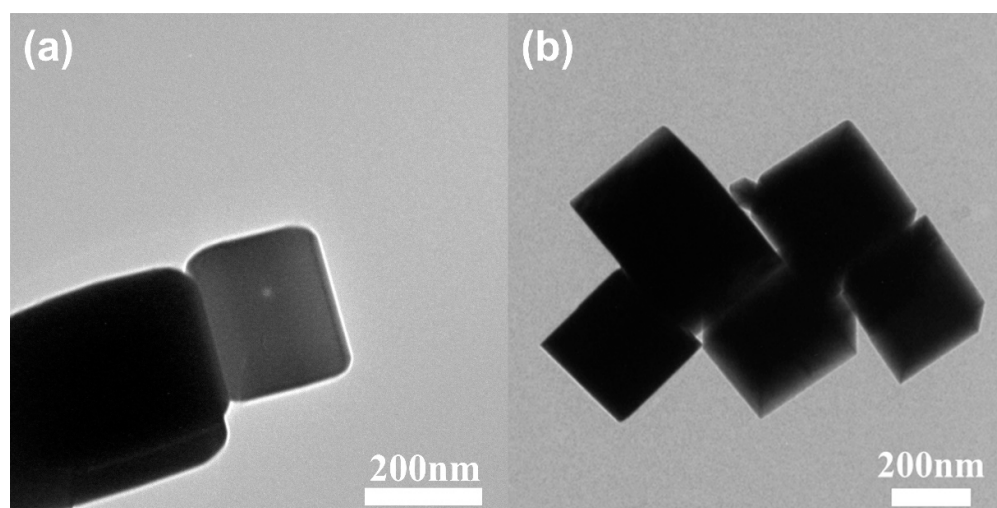

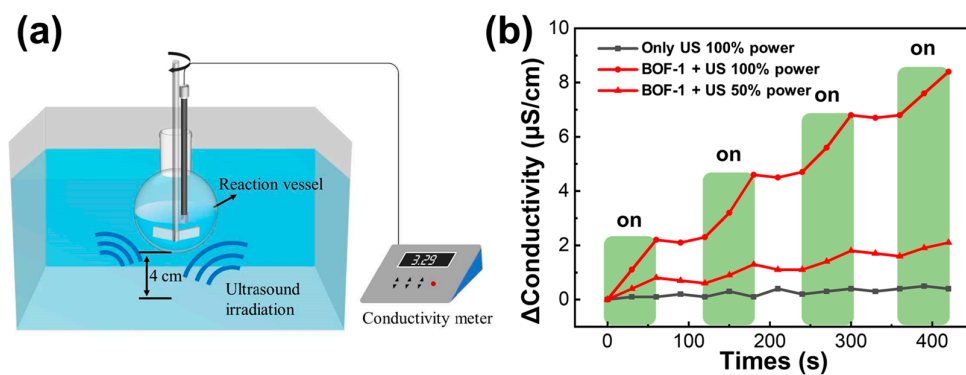**Figure S4.** TEM image of ZnO (a) and $BiFeO_3$ (b).

Figure S5. Ultrasonic-conductivity response experiment device (a) and the conductivity of BFO-1 solution increased with the ultrasonic irritated (b).
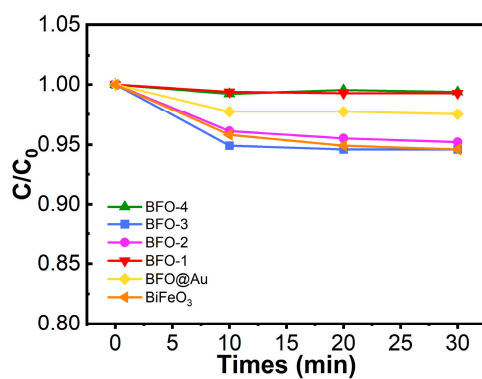

Figure S6. The concentration change of Cr (VI) in the process of adsorption-desorption equilibrium with catalysis, all experiments were carried out at 20℃ in dark environment.
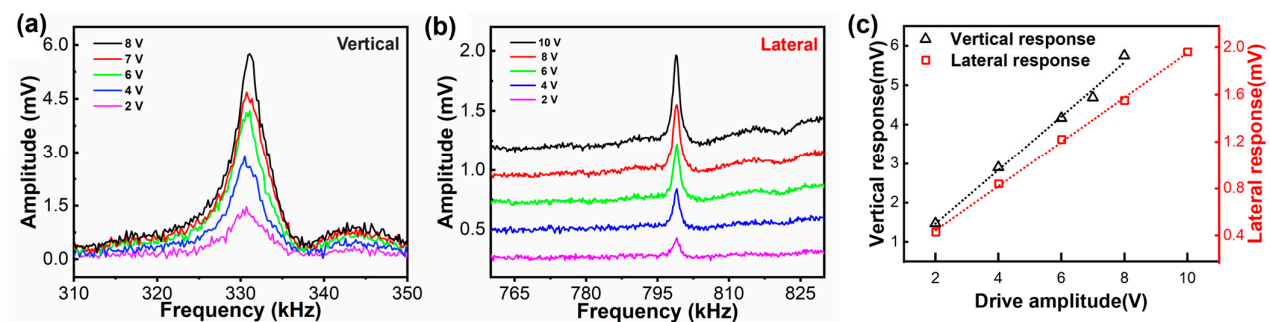

Figure S7. Vertical and lateral PFM responses of BFO-1 across resonant frequency (a,b), Resonance peaks at different applied voltages and Linear correlation between drive voltage and piezoresponse (c).
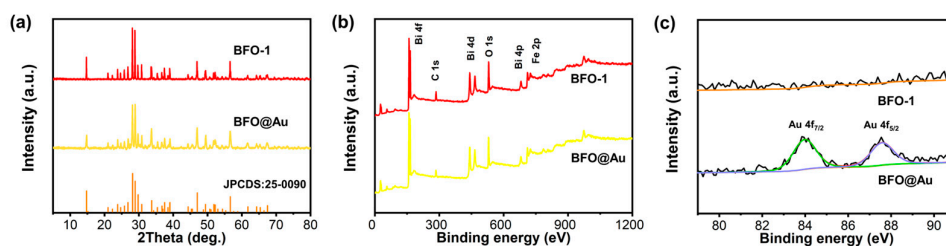
Figure S8. XRD patterns of BFO-1 and BFO@Au (a), XPS spectra of BFO-1 and BFO@Au (b) and corresponding fine peaks of Au 4f (c).
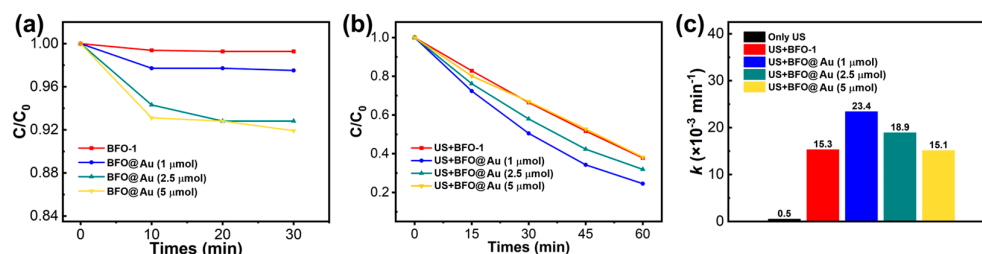

Figure S9. The concentration change of Cr (VI) in the process of adsorption-desorption equilibrium with catalysis (a), piezocatalytic reduction rate of Cr (VI) (b) and the chemical reaction rate constants of different materials.
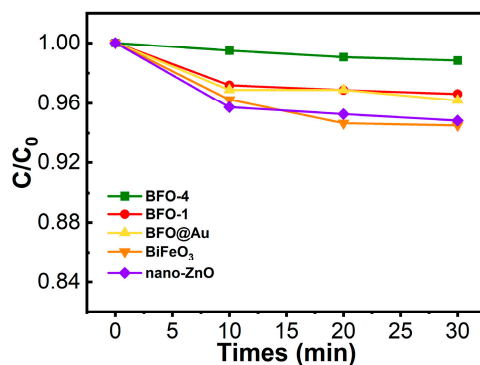

Figure S10. The concentration change of APAP in the process of adsorption-desorption equilibrium with different catalysis.

Table S1. EDS Quantitative Results on BFO materials

	Bi (Wt%)	Fe (Wt%)	O (Wt%)	Au (Wt%)	Total
BFO-1	53.39	28.41	18.20	-	100.00
BFO@Au	54.01	27.92	17.83	0.24	100.00
BFO-2	53.10	27.57	19.33	-	100.00
BFO-3	52.72	28.76	18.52	-	100.00
BFO-4	53.26	26.91	19.83	-	100.00

Reference

1. Wang, Y.; Rao, L.; Wang, P.; Shi, Z.; Zhang, L. Photocatalytic activity of N-TiO2/O-doped N vacancy g-C3N4 and the intermediates toxicity evaluation under tetracycline hydrochloride and Cr(VI) coexistence environment. *Applied Catalysis B: Environmental* **2020**, *262*, 118308.